Rapid Tracking and Cataloging Fragmentation in Orbit Using Three Telescopes: The Intelsat 33E Case

Manuel Pavy, Valentin Baral , Emmanuel Delande, and Yvan Gary
DAO/SME/ESE - CNES
18 Av. Édouard Belin, 31400 Toulouse, France
Pascal Richard
DAO/SME//SSE - CNES
18 Av. Édouard Belin, 31400 Toulouse, France
Raphaël Fermé
CS Group
6 Rue Brindejonc des Moulinais, 31500 Toulouse, France

ABSTRACT

In 2024, we witnessed two major fragmentation events in the vicinity of geostationary orbits, a critical region for various space applications. The recent fragmentation of Atlas V Centaur on Sep 6, 2024, and Intelsat 33E on Oct 19, 2024, whether due to collisions or explosions, play a major part in the current growth of space debris in the Geostationary orbit (GEO) region. These events, although rare, have significant impact on the space environment, especially at GEO altitudes where pieces of debris linger in orbit almost indefinitely.

These unfortunate events underline the critical importance of space surveillance. The timely description of the cloud of debris, and its integration to the space catalog, are essential to maintaining the safety and sustainability of space activities. Estimating the composition (size and individual states) of the cloud of debris right after its inception is paramount to the efficiency of the cataloging process, but it entails specific challenges: 1) Observing the cloud right after the fragmentation event requires specific cueing strategies of the sensor network, beyond the usual surveillance routine. 2) The measurement-to-track association is particularly ambiguous in the early stages of the cloud's lifetime, especially so since a priori information about the composition of the cloud is scarce at best.

This paper will address these two critical steps, in the context of the French orbital catalog maintained by the French Space Agency (*i.e. Centre National d'Etudes Spatiales*) (CNES).

We will first explain how, in the first nights, the system was able to acquire photos and gather information useful for the next nights with only three telescopes. This ability is based on the following principle: The sooner a fragment is cataloged; the more time we have to catalog others.

When the information about a potential fragmentation is triggered, we program the telescope to observe according to two strategies:

1. track the main body and detect other fragments,
2. follow the new observed fragments.

Then, the cataloging process tracks and characterizes the different fragments; each step will be detailed in the context of Intelsat 33E fragmentation in this paper.

1. INTRODUCTION

1.1 Presentation of Intelsat 33E

Launched in August of 2016, Intelsat 33E (fig. 1) was equipped with the most advanced digital payload on a commercial spacecraft. Intelsat 33E, operating from 60° East, extended Intelsat's HTS services in C-, Ku- and Ka-band to Europe, the Middle East, Africa, Asia Pacific, Mediterranean and Indian Ocean regions.

Fig. 1: Overview of Intelsat 33E (Credit : Intelsat)

After a phase of positioning, Intelsat 33E entered in service on 29 January 2017.

At launch, the throughput of this telecommunications satellite was expected to represent a 10-fold increase over that of previous traditional spacecraft. It therefore responded to a major connectivity challenge.

The main public information concerning Intelsat 33E is summed up in table 1.

NORAD	41748
International designator	2016-053B
Operator	Intelsat
Manufacturer	Boeing
Platform	Boeing 702MP
Launch date	24-Aug-2016
Launch site	Guiana Space Center
Launch vehicle	Ariane 5 ECA
Orbit	Geostationary / 60° E
Station keeping accuracy	±0,05° (N.S. / E.W.)
Operational life-time	15 years
Stabilization	Three axes
Payload electric power	13kW
Mass of satellite	6575 kg
Ku-band, Linear	268x36 transponders
C-band, Circular	79x36 transponders

Table 1: Intelsat 33E ID card

1.2 Presentation of french optical network (TAROT)

The fast telescope for transitory objects (*i.e. Télescope à Action Rapide pour les Objets Transitoires*) (TAROT) network [1] owned by the National Center of Scientific Research (*i.e. Centre National de Recherche Scientifique*) (CNRS) represents a main part of the French national system of Space Surveillance Awareness (SSA) and provides the brunt of the images of the GEO belt from three telescopes around the world:

1. Tarot Calern (TCa) in mainland France,
2. Tarot Chili (TCh) in Chile,
3. Tarot Réunion (TRe) in the Reunion Island (France);

To complete the GEO belt the telescope Tarot Nouvelle Calédonie (TNC), owned by CNES, entered service in 2025 and was not available at the time of the event of interest in this paper.

All the TAROT measurements are computed by a CNES software called satellites observation, measurements and orbits for Space Surveillance and Tracking (SST) (*i.e. Observation des Satellites, Mesures et Orbites pour la Surveillance de l'Espace*) (OSMOSE).

In this paper, we will explain how, by acting on each step of the chain, OSMOSE software is able to catalog dozens of new Resident Space Object (RSO) in a short time.

First, the essential pointing strategy designed to optimize telescope time utilization will be presented. Subsequently, a key automated feature for acquiring additional measurements on observed objects will be detailed. Then, the methodology for processing acquired images and cataloging fragments sequentially will be described. Finally, the results of this cataloging process will be presented.

2. POINTING STRATEGY

To effectively catalog debris from fragmentation, we have different pointing strategies available. In the case of INTELSAT 33E, we rely on two of them: track the main body and its neighborhood on one hand and observe at the fragmentation point on the other hand. This dual approach maximizes our ability to detect, characterize, and catalog the resulting debris population.

2.1 Track the main body and detect other fragments

For individual fragment observations, we implement a strategy where telescopes are pointing the object's position both before and after its true anomaly. This method, illustrated in figure 2 involves acquiring picture on the orbit position of the initial object then, depending on the field of view, acquiring picture with an orbSampleStep delay (forward and backward the initial on-track). Depending on the duration since the fragmentation, we should adapt orbSampleNb to retrieve fragments further away from the initial position on the orbit along the track.

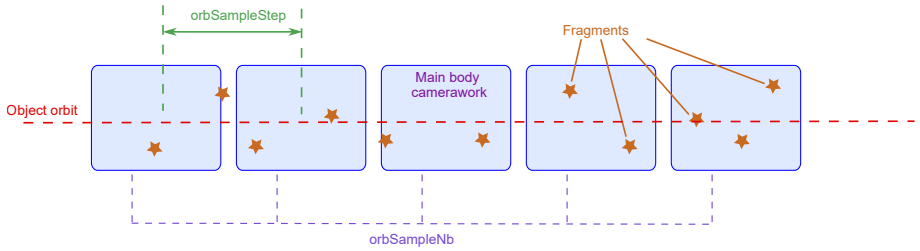

Fig. 2: *Around object* strategy pointing

This strategy is mainly effective to detect and track fragments in the original plane.

2.2 Explore fragments at the fragmentation point

In parallel, we employ a fixed-point observation strategy focused specifically on the precise orbital location where the fragmentation event occurred. This method, illustrated in figure 3 is based on the fundamental principle that all fragments will pass through the point in space where the fragmentation event took place. While the relative velocities of fragments cause them to disperse over time, they are all present at the fragmentation point immediately after the event. Our implementation involves precisely determining this fragmentation point using initial observations and orbital propagation, then scheduling repeated observations of this specific orbital location. We multiply acquisitions in order to get measurements for each fragment, even if its period has increased or decreased. By combining multiple observation passes, we build a comprehensive picture of the debris population.

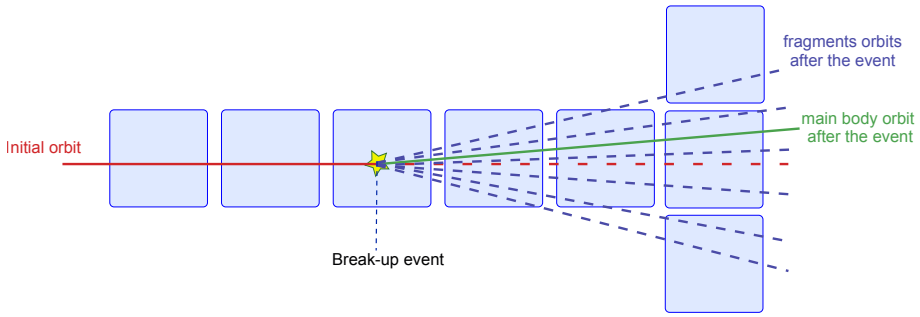

Fig. 3: *Around fragmentation* strategy pointing

This strategy is mainly effective to detect fragments out of the original plane but require more observation nights to track them.

Pointing strategy summary

The combination of *around object* and *around fragmentation* observations creates a more complete and accurate picture of the space situation, supporting both immediate operational needs and long-term space sustainability efforts.

3. MEASUREMENT ACQUISITION

In order to catalog RSOs, a substantial number of measurements must be acquired, despite the inability to perform correlation at this stage. The re-observation process, described in a previous AMOS paper [7], plays a central role in cataloging. This section describes its operational principles and shows how it fits into the larger process.

3.1 Re-observation process: reminder of the principle

The re-observation process is based on the approximation in a circular orbit of a set of measurements called tracklet (detailed in §4).

When OSMOSE can not correlate a tracklet (a set of three or more coherent measurements), it decides to re-observe the corresponding RSO assuming that this object evolves on a circular orbit. For this mechanism, it takes into account angles and the velocity.

This mechanism is particularly effective when a new RSO appears, or when the usual measurement-to-object association process fails due to a large-scale maneuver.

The temporal responsiveness of the observation system is critical for effective cataloging. Specifically, shorter the time interval between detection and scheduled observation, less the debris cloud disperses, thereby increasing the number of objects that can be observed and correlated.

3.2 Application to the break-up event

A fragmentation event, particularly in geostationary orbit, represents an ideal use case for the automated re-observation process, which can be triggered multiple times within a single night.

The image 4 shows a picture taken from a re-observation process (which will be used to catalog about sixteen new RSO):

1. this image was taken thanks to a previous re-observation process;
2. it triggers at least one re-observation pointing.

The table 2 shows some statistics on this behavior, after several new, yet-to-be-cataloged objects appeared because of the fragmentation of INTELSAT 33E.

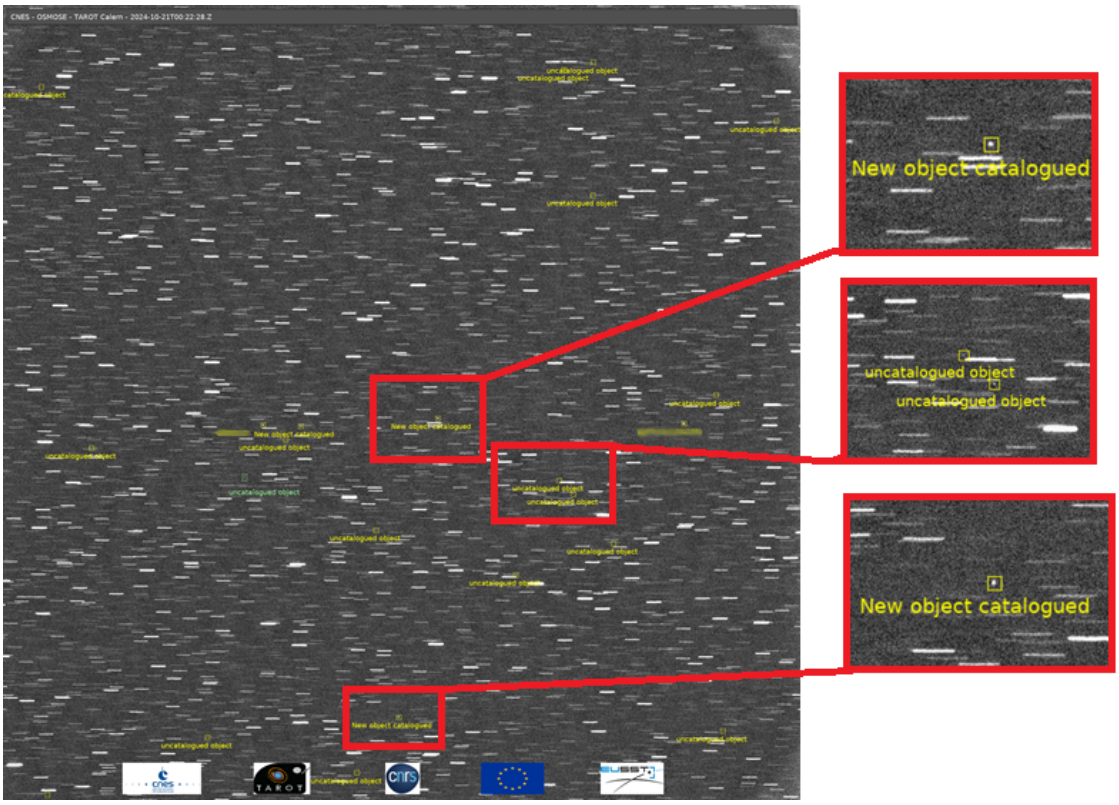

Fig. 4: Image triggered by and triggering a re-observation

Night	Number of reobs.	Number of distinct objects
2024-10-20	165	10
2024-10-21	21	8
2024-10-22	4	2
2024-10-23	103	13
2024-10-27	24	9
2024-10-28	47	12
2024-10-29	56	9
2024-10-30	10	7
2024-10-31	4	4
2024-11-01	7	5
2024-11-02	10	2
2024-11-03	6	3
2024-11-04	5	5
2024-11-05	3	3
2024-11-06	6	4
2024-11-07	23	4
2024-11-08	4	2
2024-11-09	2	2
2024-11-10	4	4
2024-11-11	6	4
2024-11-12	2	2
2024-11-14	2	1
2024-11-16	1	1
2024-11-18	3	3

Table 2: Number of re-observation processes triggered per night and number of object corresponding to RSO cataloged a posteriori

3.3 Self-feeding System

Once a re-observation acquires a new set of measurements, it should detect a new uncorrelated tracklet, triggering the mechanism once again based on the updated circular approximation. This iterative cycle can be repeated multiple times within a single night. We present a summary of the first night's observations following the INTELSAT 33E break-up event in Table 3.

The first line is particularly remarkable because 26 re-observation in 9 hours and 10 minutes correspond to a new observation every 20 minutes, or to each occurrence of a photo of the processed track.

Once enough occurrences of reobsevation have been triggered, the system can rebuild the chain of all the measurements from a recursive query involving each tracklet built thanks to the re-observation of a previous tracklet. At this point, an orbit restitution is attempted and if it succeeds, a new RSO is added into the catalog as an unknown object.

This object is then tracked using the same methodology as all other cataloged RSOs.

In practice, each re-observation provides an uncorrelated measurement which generates new re-observation, until an orbit is built and an object entered into the catalog.

Number of reobs occurrences	First measurement	Last measurement
26	2024-10-20 19:25:26	2024-10-21 03:46:25
22	2024-10-20 18:09:23	2024-10-21 01:43:35
16	2024-10-20 19:26:51	2024-10-21 01:40:39
21	2024-10-20 18:10:54	2024-10-21 03:14:14
5	2024-10-20 18:44:14	2024-10-21 00:23:30
19	2024-10-20 19:03:33	2024-10-21 00:56:26
24	2024-10-20 20:21:58	2024-10-21 03:20:09
3	2024-10-20 21:12:52	2024-10-21 00:02:58
3	2024-10-20 21:58:25	2024-10-21 01:46:26

Table 3: Recursive re-observation process in the first night per track

Please note: The sum of fragments found does not correspond to the number of distinct objects; sometimes the re-observation process spread over several nights, sometimes also, objects can be lost then found again.

Once the system is auto feeding, we can retrieve the coherent tracklets which have been built from recursive re-observation pictures.

4. EXPLOIT UNCORRELATED TRACKLETS

To improve cataloging efficiency, we implement an orbital plane segregation strategy that organizes RSOs and uncorrelated tracklets based on their circular approximation orbit parameters. This section describes the methodology and presents a practical use case.

4.1 Orbital plane segregation

To find new RSOs is, once a large number of observations and detections have been acquired, to determine which detection groups are correlated with each other.

As described in the previous paper [7], the OSMOSE system uses groups of detections as tracklets. For each tracklet, an approximated circular orbit is computed and is defined with these parameters:

- a: semi major axis
- $\vec{h} = \begin{pmatrix} \tan(\frac{i}{2})\cos(\Omega) \\ \tan(\frac{i}{2})\sin(\Omega) \end{pmatrix}$: the orbital plane, removing the ambiguity on the position of the right ascension node
- l: the projected longitude

As moving from an orbital plane to another requires a certain amount of energy, we can consider that once the fragmentation happened, the objects individually evolve in their own (new) plane and during a short period, the vector $\vec{h}$ is constant.

For a longer period, we should consider the natural evolution of the vector $\vec{h}$, taking into account the lunisolar potential, tesseral terms and solar pressure (this last effect depends on the object's characteristics) [3].

From the track detected as a recursive circular approximated orbit, an orbit determination is attempted. If it converges, a new RSO is added into the catalog with the status 'TO_BE_CONFIRMED'; if it does not converge, the system analyzes some other characteristics like magnitude, the number of measurements per tracklet,... to apply other filters before proceeding to a new attempt. In any case, new observations are requested to the TAROT network to provide complementary measurements.

4.2 Practical example

To illustrate the segregation of the orbital plane, the graphic 5 shows the evolution of all tracklets built by the OSMOSE system, filtered by the orbital plane of an uncorrelated tracklet (real case). This figure is produced for each uncorrelated tracklets, each day.

This example attests that, since a filter on h_x and h_y is done (and their values are quite far from the perfect equatorial plane), there are very few objects evolving in that plane and distinct tracks can emerge.

In this example, the selected plane is $h_x \in [-0.0148, -0.0128]$ and $h_y \in [0.0091, 0.0111]$. These intervals are choosen as the classical margin around an unknown tracklet.

In this plane, the graph displays:

- 5 known and already cataloged object (magenta, blue, pink, green and black markers)
- 6 uncorrelated isolated tracklets with red and numbered markers. These may be false detections or objects that are difficult to observe.
- 1 emerged track (ocher markers with numbers in orange background)

From the emerged track, the system is able to automatically attempt an orbit determination using all measurements and, if the orbit determination is considered as valid by OSMOSE, adds a new unknown object in the catalog awaiting confirmation by series of future observations.

In the example chosen to illustrate the explanation, although real, the uncorrelated track is particularly easy to detect. In the operational system, it is often less obvious.

If the generated graph contents too many objects, known RSOs are filtered and only emerged tracks and alone tracklets are displaying.

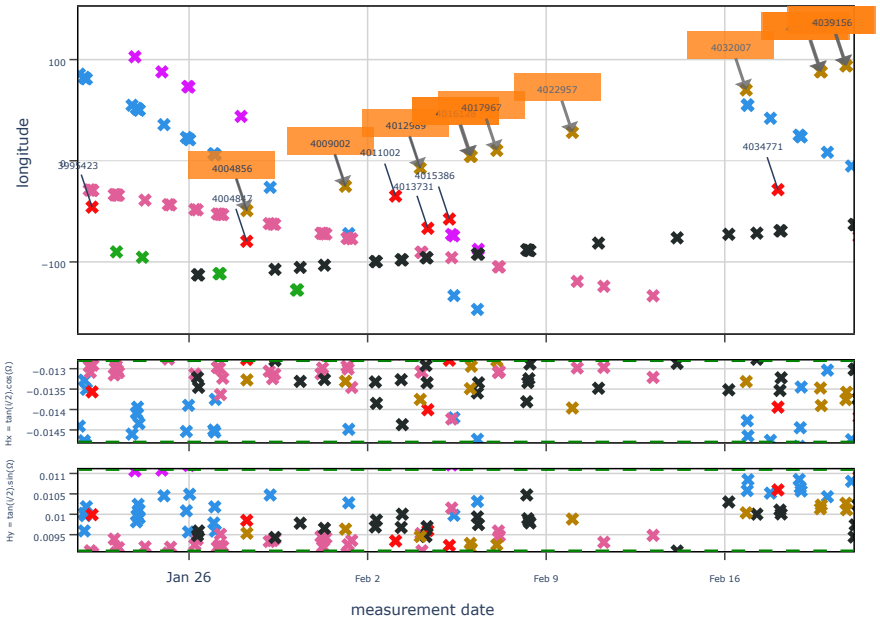

Overview of objects in a specific orbital plane over one month.

- **Known objects**: magenta, blue, pink, green, and black markers.
- **Isolated and uncorrelated tracklets**: red markers with with annotation of numbers.
- **Emerged tracks**: ocher markers with annotation of numbers on an orange background.

Fig. 5: Example of plane segregation with $h_x \in [-0.0148, -0.0128]$ and $h_y \in [0.0091, 0.0111]$.

5. RESULTS AND IMPROVEMENT

The implementation of our observation and re-observation strategies has yielded significant improvements in fragments cataloging and characterization. This section presents an overview of these results and introduces the benefit of an architectural improvement made since INTELSAT 33E fragmentation.

5.1 Fragmentation cataloging overview

The method to associate an unknown object with a fragmentation event involves retro-propagating its orbit to identify a temporal and spatial coincidence with the main body's trajectory.

Three days after the break-up event, CNES had already cataloged 40 fragments. After 100 days, it reached to 80 fragments. To date, the catalog process is keeping track of around 100 objects resulting from the fragmentation of Intelsat 33E.

As figure 6 shows, this event triggered many observations in order to follow these objects correctly. Tracking is difficult due to the tumbling effect which causes:

1. variable SRP resulting in perturbations in the trajectory dynamics
2. variable magnitude leading to difficulties in correlating observed detections and objects in the catalog or recent revealed tracks
3. non detection in some observations can stop the re-observation chain of a newly detected fragment.

4. by extension, once a tracking is stopped and the dynamics are poorly modeled, another RSO may appear and trigger work to identify its origin and the existence of a duplicate.

Once the debris population knowledge is stabilized, CNES uses the TAROT network to keep track of the objects and apply the following independent routines :

1. Orbit Determination (keplerian parameters), and dynamical parameter such as mean solar radiation coefficient and drag when it is applicable (which is not in that case)
2. Optical Size Estimation Model (OSEM) [2][1]

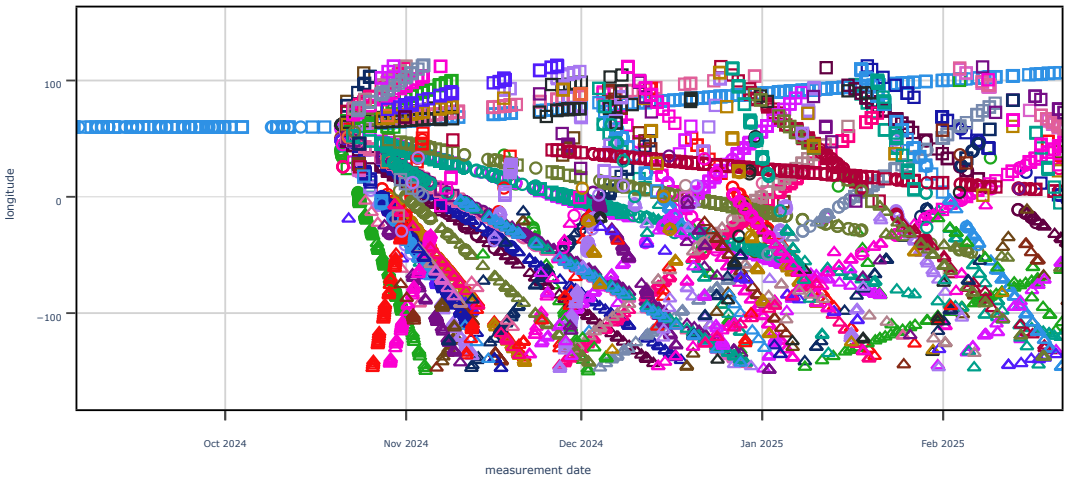

Fig. 6: Overview of the evolution of cataloged fragments through longitude

From these automated computed data, area, volume and mass can be normalized to the OSEM size (designated with OSEM indices). The reader should take note that this approach is based on a simplistic model that will not represent each object's physical properties with a high level of fidelity.

In this context, for each fragment, its OSEM normalized volume is computed by:

$$\mathrm{V}_{\mathrm{OSEM}_i} = \frac{4}{3} \cdot \pi \cdot \left(\frac{\mathrm{D}_{OSEM_i}}{2} \right)^3 \tag{1}$$

and the OSEM normalized mass is done by:

$$\mathrm{m}_{\mathrm{OSEM}_i} = \frac{\pi \cdot \left(\frac{\mathrm{D}_{\mathrm{OSEM}_i}}{2} \right)^2}{\mathrm{srp}_i} \tag{2}$$

In the graphic 6, cataloged objects after 100 days are presented in different color (only fragments with at least six months of continuous data are considered in this paper). They are also detailed in table 5, appendix A.

[1]OSEM is computed based on a Lambertian spherical phase function correction to zero degree phase angle and an albedo of 0.1

	V_{OSEM}	m_{OSEM}
N41748	454.6	3409
$\sum fragments$	210.4	3296
$\Delta_{before/after}$	244.2	112.8

Table 4: Sum up mass and volume before and after break-up

In complement, Table 4 provides an overview on OSEM normalized mass and volume. We can notice that the total of OSEM normalized mass of all fragments is quite close to the OSEM normalized mass of the initial object. It misses about one hundred thirteen kilograms-OSEM. Probably a large amount of fragments is not included because they are not detectable by the three on ground TAROT telescopes or we do not have enough data to determine their characteristics with confidence; either propellants may have burned but the main reason is that the modeling is greatly simplified. Such results should be regarded as indicative of cataloging performance rather than as conclusive evidence of completeness. Indeed, the diverse composition of the fragments results in varying reflectance characteristics. Although statistical averaging helps to mitigate these variations to a certain degree, the non-spherical nature of the fragments introduces inherent challenges in the characterization process. Nevertheless, this approach offers meaningful contributions to our understanding of the fragmentation phenomenon.

5.2 *Time of Closest Approach* dispersion

The main difficulty to the orbit determination is that fragments are not homogeneous neither spherical. Nevertheless, we have enough data to evaluate, for each fragment, this Time of Closest Approach (TCA). For that, we retro-propagate all orbits and check the time the object is the closest to the orbit of the initial object (by propagation of the last known orbit).

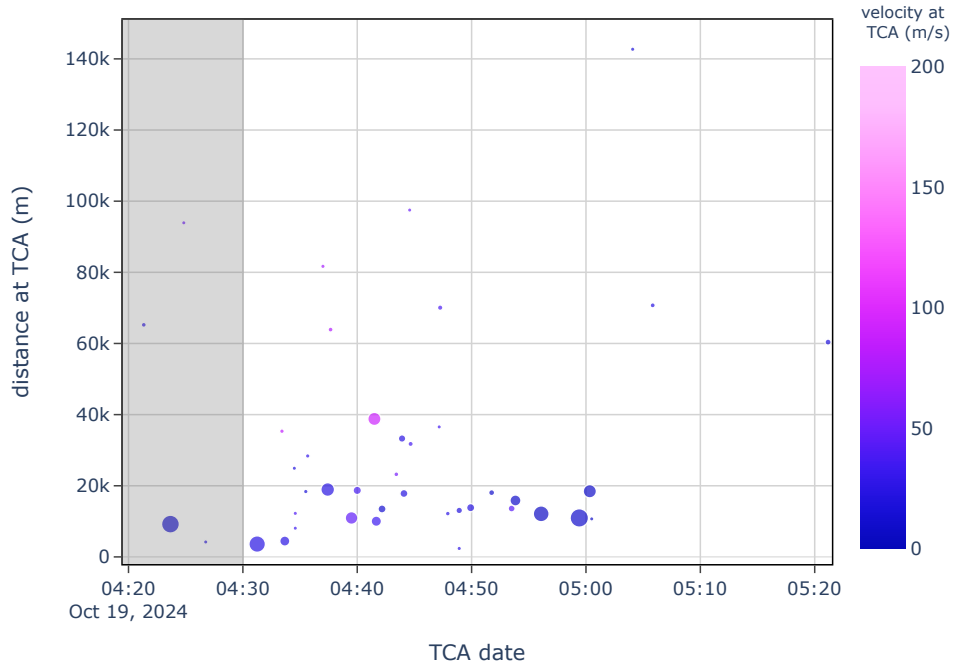

This plot presents a temporal and dynamical analysis of fragments resulting from the INTELSAT 33E fragmentation. Each point corresponds to a fragment:

Axes:

- **X-axis (Abscissa)**: Date and time (UTC) corresponding to the closest moment of fragment separation, computed through orbital propagation or retro-propagation.
- **Y-axis (Ordinate)**: Distance computed between the main body and the fragment (in meters).

Data Representation:

- **Point size**: Normalized OSEM mass.
  - Larger points indicate higher fragment mass.
- **Point color**: Computed Delta-V (ΔV) between the main body and fragment orbit (in m/s).
  - Color scale from blue (low ΔV) to pale pink (high ΔV) represents relative velocity between trajectories.
- **Sign of life**: Grey area is excluded to the real date of the break up
  - Passive ranging data indicates the satellite was transmitting until 04:30 UTC on October 19Th.

Fig. 7: TCA analysis of INTELSAT 33E fragments

Through this exercise we can check how the orbit determination is correct by representing all these TCA in figure 7. In addition, from this computation, we can determine which objects is the consequence of the break up occurred on INTELSAT 33E satellite (because we also acquired several RSOs due to another fragmentation a month earlier, that of the rocket body ATLAS V Centaur, NORAD 43227).

5.3 Sensor evolution

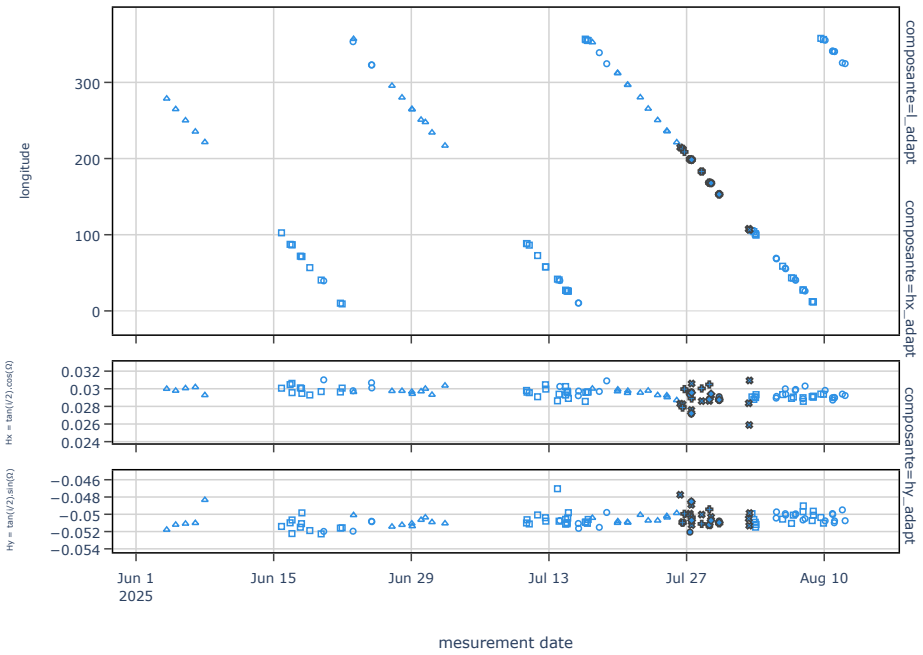

Fig. 8: The fourth telescope in New Caledonia closed the GEO observational gap by precisely monitoring a debris object in the upper GEO region.

Since June 2025, a new optical surveillance telescope located in New Caledonia has been progressively integrated into operational service [6]. As depicted in Figure 8[2], this strategic installation constitutes a breakthrough improvement in the monitoring architecture of the GEO region, complementing and enhancing the capabilities of the existing TAROT network.

The telescope's strategic positioning in the South Pacific region addresses a persistent observational gap that previously limited comprehensive coverage of the GEO belt. This gap was particularly problematic for tracking objects in the upper GEO region, where the TAROT network's coverage exhibited inherent limitations. The new facility's advanced instrumentation and optimized field of view enable precise detection and characterization of RSO in this critical orbital regime.

The enhanced observational capabilities are particularly crucial given the significant challenges in cataloging and tracking RSOs in GEO. These challenges stem from several key sources of uncertainty:

- **Maneuver-related uncertainties**: station-keeping maneuvers or mission maneuvers by operational satellites make orbital predictions unreliable and in turn hamper the correlation of observed tracks with known RSOs.
- **Attitude determination uncertainties**: The orientation of objects in GEO significantly affects their Solar Radiation Pressure (SRP) coefficient, which is a dominant perturbation force in this orbital regime. Variations in attitude can lead to orders-of-magnitude differences in SRP-induced accelerations, creating substantial orbit determination errors.

While the increased observational capacity naturally results in a higher volume of data requiring sophisticated processing algorithms and analytical methodologies, this expansion represents a net operational advantage. The enhanced data

[2]This graph represents longitude from 0° to 360° to call attention on the gap between 100° and 210°

stream facilitates more robust association of unknown objects with the catalog through advanced orbit determination techniques, including precise retro-propagation and temporal-spatial proximity analysis.

The telescope's contributions are especially significant given the critical nature of the GEO belt, which hosts approximately five hundred operational satellites providing essential communication, broadcasting, and meteorological services. By reducing the observational gap, this new asset enhances our ability to maintain spatial situational awareness.

The deployment of the new optical surveillance telescope in New Caledonia constitutes a major advancement in our capacity to monitor and catalog RSO within the geostationary equatorial orbit (GEO) regime. While the present study has focused on the well-documented INTELSAT 33E fragmentation event, the telescope's enhanced observational capabilities will enable future research to address previously unresolved object associations that were excluded from catalogs due to uncertainties.

This work establishes a critical foundation for ongoing and future research efforts. The continuous enhancement of our observational infrastructure, coupled with sophisticated data processing methodologies, will facilitate more comprehensive and precise characterization of the GEO environment. The ability to systematically track and analyze previously ambiguous objects will prove particularly valuable to:

- Re-examine previously uncertain object associations with improved confidence levels
- Incorporate marginal observations that were previously excluded due to insufficient data
- Develop more robust algorithms for handling objects with high uncertainty parameters
- Enhance space traffic management capabilities with better characterized objects
- Support long-term space sustainability efforts through more accurate cataloging

As our understanding of the GEO environment continues to evolve, this new telescope will play a crucial role in maintaining an accurate and exhaustive catalog of resident space objects, ultimately contributing to the safety and sustainability of space operations.

6. CONSEQUENCE ON THE COLLISION AVOIDANCE SERVICE

The fragmentation event and the resulting increase in debris population have introduced significant risks to operational satellites in the GEO regime.

The proliferation of debris fragments creates multiple operational challenges:

- **Conjunction**: Increased probability of close approaches between debris objects and operational satellites
- **High mitigation action rates**: Additional burden on satellite operators to perform avoidance maneuvers
- **Long-term sustainability concerns**: Potential for cascading fragmentation events that could further degrade the GEO environment (Kessler syndrome [4])

The french team in charge of collision avoidance for European Union Space Surveillance and Tracking (EUSST) uses Java for Assessment of Conjunction (*i.e. the conjunction software used by French EUSST collision avoidance team*) (JAC) software to analyze Conjunction Data Message (CDM).

As illustrated in Figure 9, the JAC monitoring data filtered for secondary debris objects clearly demonstrates the consequences of this fragmentation event. A operational case even engendered a maneuver due to critical risk with CoPOC $> 10^{-4}$ as displayed on Fig 10.

This analysis underscores the critical need for enhanced space situational awareness capabilities in GEO, particularly in light of the growing debris population.

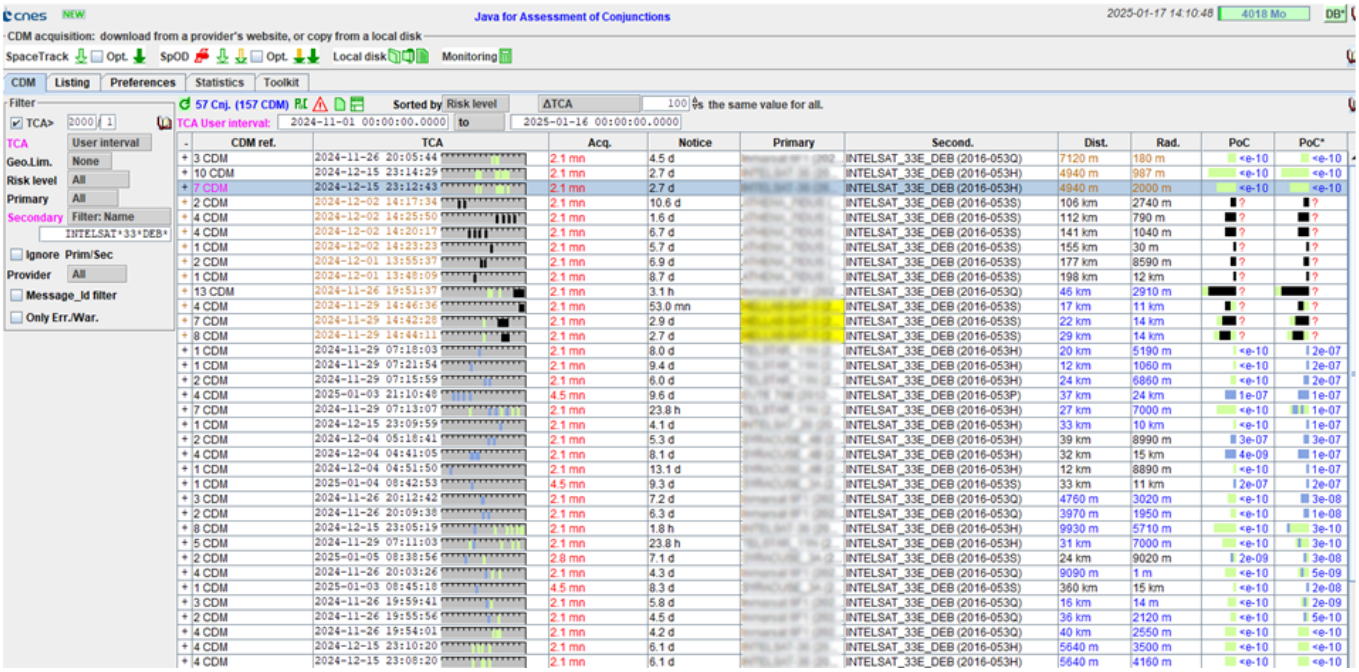

Fig. 9: Overview of JAC [5], involved new fragments detected, 10 days after event

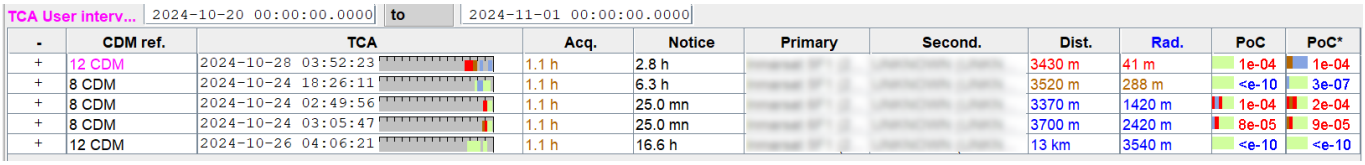

Fig. 10: Cases of critical conjunction events requiring orbital adjustment maneuver

7. CONCLUSION

This study presents a comprehensive methodology for the rapid characterization and cataloging of fragmentation debris in geostationary orbit, demonstrated through the analysis of the Intelsat 33E breakup event. Our approach leverages a multi-telescope observation network and sophisticated data processing techniques to address the complex challenges associated with space debris monitoring.

The implementation of dual observation strategies - comprising both main body tracking and fragmentation point observation - has proven effective in maximizing fragment detection. The iterative re-observation process, with its optimized temporal responsiveness, enables the progressive construction of fragment trajectories through the circular orbit approximation technique. This methodology is particularly effective in the critical initial phase following fragmentation events, where traditional tracking methods often face significant limitations.

Our methodology also demonstrates excellent reactivity in debris cataloging, successfully determining orbits of 40 fragments within 72 hours of the Intelsat 33E breakup - a critical window where most systems struggle to establish such reliable tracking. This rapid response capability is fundamental to our approach, enabling the cataloging of fragments before significant dispersion occurs.

The iterative re-observation process, with its optimized temporal responsiveness, allows for progressive refinement of fragment trajectories through circular orbit approximation. After 100 days, our system has cataloged 80 fragments, outperforming previous systems.

The superior performance of our system is evidenced by its ability to maintain continuous tracking of fragments over extended periods, enabling refined orbital parameter assessment and long-term debris evolution monitoring -

capabilities that represent significant improvements.

The recent incorporation of a fourth telescope in New Caledonia has significantly enhanced our observational capabilities, particularly for objects in the GEO region. This expansion addresses a critical gap in our surveillance architecture and enables more comprehensive monitoring of the geostationary belt. The improved spatial coverage, combined with our advanced tracking algorithms, facilitates more accurate orbit determination and reduces the uncertainty in fragment characterization.

The study highlights several persistent challenges in space debris monitoring, including the variability of solar radiation pressure coefficients due to object tumbling and the difficulties in correlating observations of non-spherical fragments. These challenges necessitate continued refinement of our orbit determination algorithms and the development of more sophisticated debris characterization models.

Finally, this study expose the consequence on collision avoidance service and space environment sustainability.

These results together support the IADC's efforts in preventing collisions in orbit, taking into account the most complete catalog available by adding all the fragments detected and whose orbits could be computed.

In conclusion, this work demonstrates the effectiveness of our multi-faceted approach to space debris monitoring and cataloging. The methodologies and results presented here contribute significantly to the field of space situational awareness and provide a robust foundation for future advancements in space debris characterization and management. The continuous improvement of our observational infrastructure and analytical techniques will be crucial for maintaining the safety and sustainability of space operations in the increasingly congested geostationary orbit regime.

8. ACKNOWLEDGMENT

The first three TAROT telescopes are owned by the CNRS.

The authors would like to thank the European Union, as both the TAROT and OSMOSE projects are partially funded by the EUSST program. Warm thanks are also due to the crews of the observatories at le Calern, les Makes and la Silla for their help in shaping TAROT into a reliable and potent tool.

9. REFERENCES

[1] Michel Boër, Alain Klotz, Romain Laugier, Pascal Richard, Juan Carlos Dolado Pérez, Laurent Lapasset, Agnès Verzeni, Sébastien Théron, David Coward, and J.A. Kennewell. TAROT: a network for space surveillance and tracking operations. In *7th European Conference on Space Debris ESA/ESOC, Darmstadt/Germany*, Darmstadt, Germany, April 2017. ESA.

[2] GE Bohannon and N Young. Debris size estimation using average rcs measurements. Technical report, Report, 1993.

[3] G. Campan, F. Alby, and H. Gautier. Les techniques de maintien à poste de satellites géostationnaires. *CNES, Mécanique spatiale*, Tome II:983–1085, 1995.

[4] Donald J Kessler and Burton G Cour-Palais. Collision frequency of artificial satellites: The creation of a debris belt. *Journal of Geophysical Research: Space Physics*, 83(A6):2637–2646, 1978.

[5] François Laporte. Jac software, solving conjunction assessment issues. In *Advanced Maui Optical and Space Surveillance Technologies Conference*, page E4, 2014.

[6] Vincent Morand and Sylvain Delattre. Cnes space surveillance office latest advancements in support of the safety, security, and sustainability of space operations. *LPI Contributions*, 2852:6081, 2023.

[7] Manuel Pavy, Pascal Richard, Emmanuel Delande, and Sébastien Théron. Improving the operational signal processing chain for faster acquisition of new objects to the french national catalogue of orbital objects. In *Proceedings of the Advanced Maui Optical and Space Surveillance (AMOS) Technologies Conference*, 2023.

[8] Pascal Richard, Carlos Yanez, Vincent Morand, Agnès Verzeni, Michel Boer, and Alain Klotz. Exhaustive strategy for optical survey of geosynchronous region using tarot telescopes. In *Proceedings of the AMOS Technical Conference*, 2017.

ANNEXES

A. FRAGMENTS AND CHARACTERIZATION

Object ♯	OSEM diameter	OSEM volume	SRP	$mass_{\mathrm{OSEM}}$
N41748	10.5	454.60	0.0254	3409.06
63559	4.55	37.01	0.011	1462.55
85150	1.05	0.45	0.050	17.21
85151	1.01	0.41	0.048	16.89
85152	1.74	2.06	0.048	48.88
85154	2.42	5.58	0.410	11.24
85155	1.64	1.73	0.076	27.83
85156	1.82	2.35	0.042	61.64
85157	1.48	1.27	0.033	51.43
85158	2.16	3.98	0.014	265.61
85160	2.37	5.24	0.011	384.88
85161	3.19	12.74	0.112	71.39
85162	2.02	3.25	0.166	19.39
85163	1.68	1.85	0.148	14.90
85176	1.58	1.55	0.087	22.46
85183	1.02	0.41	0.005	160.16
85185	0.93	0.31	0.081	8.38
85188	1.79	2.25	0.026	94.94
85193	0.90	0.29	4.381	0.15
85194	0.75	0.16	0.113	3.86
85196	5.08	51.46	2.095	9.67
85197	1.05	0.45	1.399	0.62
85204	1.59	1.57	0.328	6.03
85222	1.60	1.62	0.087	23.28
85225	0.53	0.06	0.573	0.38
85226	1.57	1.53	0.109	17.73
85244	1.63	1.71	0.043	48.47
85246	1.38	1.03	3.479	0.43
85247	1.55	1.47	0.092	20.58
85299	0.90	0.29	0.229	2.81
85300	1.52	1.38	4.192	0.43
85305	0.97	0.36	1.122	0.66
85307	1.24	0.74	3.832	0.31
85308	1.22	0.72	0.052	22.59
85310	1.76	2.12	0.078	31.06
85311	0.85	0.24	4.242	0.13
85360	1.20	0.67	0.063	17.72
85363	2.72	7.88	0.337	17.19
85364	1.72	2.00	0.051	45.32
85365	1.66	1.80	0.216	10.02
85470	1.33	0.93	0.560	2.50
85475	1.84	2.45	0.402	6.63
85476	0.62	0.09	0.017	17.90
85533	0.42	0.03	0.327	0.42
85572	1.47	1.24	0.159	10.59
85579	0.87	0.26	4.302	0.14
85583	0.90	0.29	0.903	0.70
85628	1.58	1.55	2.311	0.85
85653	1.28	0.82	1.152	1.11
85674	1.67	1.84	0.790	2.78

85864	1.09	0.50	0.705	1.31
85869	0.70	0.13	0.911	0.42
85874	1.29	0.84	3.402	0.38
85924	0.62	0.10	0.019	16.38
85925	0.71	0.14	0.075	5.33
85933	2.26	4.55	3.605	1.12
85934	0.80	0.20	0.031	15.90
85935	0.80	0.20	1.471	0.34
86050	0.63	0.10	0.043	7.15
86058	1.61	1.62	3.856	0.52
86063	0.85	0.24	2.797	0.20
86212	2.47	5.95	9.227	0.52
86281	0.88	0.27	0.071	8.54
86282	0.98	0.37	0.562	1.34
86283	2.35	5.08	9.667	0.45
86289	1.06	0.47	0.089	10.03
86366	0.99	0.38	0.579	1.33
86399	0.97	0.36	0.072	10.28
86529	0.64	0.10	0.297	1.07
86530	0.93	0.32	0.714	0.96
86590	1.83	2.40	0.131	20.07
86593	1.19	0.66	0.018	61.72
86594	1.18	0.64	0.127	8.53
86595	0.79	0.19	0.361	1.35
86596	0.53	0.06	0.063	3.50
86646	1.10	0.52	4.235	0.22
86664	0.71	0.14	0.019	21.66
86691	1.04	0.44	0.090	9.46
87004	1.30	0.87	5.463	0.24
87008	0.64	0.10	0.344	0.93
87036	0.53	0.06	0.025	8.66
87135	0.67	0.12	0.045	7.91
87449	1.09	0.51	2.249	0.42
87450	0.66	0.11	1.575	0.21
87644	1.33	0.92	0.533	2.59
88471	2.86	9.22	2.664	2.42

Table 5: Physical values for each object